

A microscopical examination of the gastric morphology of the white-tailed rat *Mystromys albicaudatus* (Smith 1834)

A.H. Maddock and M.R. Perrin

Department of Zoology and Entomology, Rhodes University, Grahamstown

A study of the gastric morphology of *Mystromys albicaudatus* revealed a sacculated stomach with a papillated, keratinized corpus separated from a distal glandular antrum by a pre-gastric pouch. Gastric morphology of this type is defined as bilocular hemiglandular. Although the forestomach of *M. albicaudatus* bears a superficial resemblance to that of a ruminant, the corpus (and papillae in particular) differ structurally and functionally from the rumen. Whereas rumen papillae are important in absorption, those of *M. albicaudatus* increase surface area for the attachment of symbiotic bacteria.

S. Afr. J. Zool. 1981, 16: 237 – 247

'n Studie van die gastriese morfologie van *Mystromys albicaudatus* het 'n sakvormige maagstruktuur getoon; 'n pre-gastriese sak het 'n met papillae uitgevoerde gekeratini-seerde corpus geskei van 'n distale klierryke antrum. Gastriese morfologie van hierdie tipe word gedefinieer as tweesakkig-hemigeklierd (bilocular hemiglandular). Alhoewel die voormaag van *M. albicaudatus* 'n oppervlakkige ooreenkoms toon met dié van 'n herkouer, is die corpus (en die papillae spesifiek) struktureel en funksioneel verskillend van die rumen. Papillae van die rumen is belangrik vir absorpsie terwyl dié van *M. albicaudatus* groter vashegtingsarea bied vir die simbiotiese bakteriese bevolking.

S.-Afr. Tydskr. Dierk. 1981, 16: 237 – 247

Comparative gross morphological studies of Muroid digestive systems have indicated great structural diversity (Vorontsov 1962; Carleton 1973; Perrin & Curtis 1980). A 'primitive', monogastric stomach and an 'advanced', digastric stomach (with reduction of glandular compared to keratinized epithelium) have been recognized as end points of an evolutionary continuum. Gastric morphology of most rodents examined conforms to this series but a few species show atypical adaptations. For example, *Mystromys albicaudatus* shows the digastric condition but possesses numerous papillae in the proximal, keratinized region of the stomach (Perrin & Curtis 1980); similarly, *Cricetomys gambianus*, has gastric papillae (Caiman, Quenum, Kerrest & Goueffon 1960). The gastric histology and ultrastructure of these species have not been examined and the functions of the papillae are unknown. A microscopical examination of the gastric morphology of *M. albicaudatus* was therefore initiated to determine its histology and ultrastructure, prior to studies of assimilation efficiency and microbial function.

The alimentary tract of *M. albicaudatus* is indicative of a herbivorous/omnivorous diet (Perrin & Curtis 1980). A shift in the diet of certain rodents, from omnivory (Lantry 1970) or granivory/insectivory (Vorontsov 1962) to herbivory has been associated with climatic and vegetation changes during the Miocene (Vorontsov 1962; Moir 1968). During this dry period forests were replaced by savannah and steppe vegetation (Moir 1968) causing taxa to adopt herbivorous specializations and thereby reducing interspecific competition. This change was facilitated by various anatomical, physiological and behavioural adaptations (Vorontsov 1962) including sac-culation of the stomach, an increase in keratinized epithelium and a decrease in glandular epithelium (Vorontsov 1962; Carleton 1973). Similar modifications in *M. albicaudatus* have been recorded (Perrin & Curtis 1980). In the light of the present detailed study it seems plausible to suggest that such modifications reflect an ability to digest an increasingly herbivorous diet while retaining the ability for proteolytic activity.

Materials and Methods

Adult *M. albicaudatus* were killed by chloroform anaesthesia and placed on ice to retard autolysis. Stomachs, including approximately 1 cm of the oesopha-

A.H. Maddock* and M.R. Perrin

Department of Zoology and Entomology, Rhodes University,
Grahamstown 6140

*To whom correspondence should be addressed

Received 8 May 1980; accepted 8 May 1981

gus and duodenum, were removed, cleaned of gut contents and placed in either Bouin's fixative or 10% formalin. The contents of the corpus and antrum were separated, mixed with 20 ml distilled water and the pH measured with a Beckman 3500 digital pH meter.

A dissecting microscope was used to examine gross morphology and photographs were taken with a Nikon F2 camera and 55-mm lens. Stomach dimensions were measured with calipers, and micro-anatomical features with a Leitz micrometer. A punch was used to obtain discs of papillated epithelium of 1.3-cm diameter. Papillae on the discs were counted.

Paraffin embedded material was processed, and sections 7 μ m thick were cut. Frozen sections fixed in Bouin's fluid were sectioned on a freezing microtome. General purpose tissue stains were used when examining the gastric epithelium, and specific histochemical stains when examining the non-glandular corpus (Table 1). Photographs were taken through a Wild M 400 Photomicroskop or a Vanox microscope fitted with an Olympus C 35 camera.

Table 1 Stains used when examining the gastric histology of *M. albicaudatus*

Stain	Tissue stained	Reference
Hematoxylin & eosin	General purpose, nuclear material	1
Hematoxylin alum	Nuclear material	2
Toluidene blue	General purpose, mucin	1
Feulgen	Nuclear material	1
Oil red O	Lipid	1
Sudan black B	Lipid	3
Periodic acid Schiff	Mucopolysaccharides	1
Aldehyde fuchsin	Sulphur groups	1
Ferric ferricyanide	Reducing substances	1
Aniline blue, Orange G	Keratin	4

1	Humason 1967	3	Sumner & Sumner 1969
2	Luna 1968	4	Ayoub & Skhlar 1963

Additional blocks of tissue were fixed in 5% cold buffered glutaraldehyde for a minimum of 12 h. Tissue used for scanning electron microscopy (SEM) was critical point dried (Anderson 1951), coated with gold palladium and examined with a JEOL JSM/VS scanning electron microscope. Secondary fixation and embedding of the tissues used for transmission electron microscopy (TEM), followed the procedure of Cross (1979). Sections were cut on an LKB mark 3 ultramicrotome and stained with uranyl acetate and lead citrate (Cross 1979). A Hitachi HU/11B transmission electron microscope was used to examine the sections.

To facilitate surface examination of the corpal epithelium, and to determine bacterial/epithelial associations, conventional (normal gastric flora), sterile (bacteria-free stomach) and specially treated rats (reduced gastric flora) were used (Table 2).

Results

Gross morphology

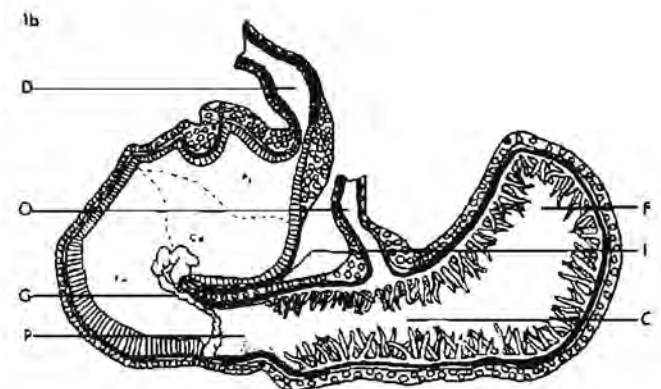
The stomach of *M. albicaudatus* was markedly sacculated (Figure 1) and differed from Carleton's (1973) 'primitive'

Table 2 Antibiotic treatment of the alimentary flora of *M. albicaudatus*

Rat treatment	Food and water
Conventional	Tap water, pelleted food
Sterile	100 mg oral oxytetracycline per day for 5 days. Pellets and water were autoclaved.
Specially treated	50 mg oral oxytetracycline per day for 5 days. Tap water, pelleted food.



Figure 1a Photograph of a bisected stomach of *M. albicaudatus* illustrating gross morphology. Insets: sections through (right) oesophageal sphincter and (left) duodenal sphincter. To avoid confusion, anatomical terms used in this paper are defined as follows: C = corpus — proximal region of stomach including the fornix ventricularis. P = pre-gastric pouch — non-glandular epithelium separating the corpus and antrum. A = antrum — distal glandular region of stomach. F = fornix ventricularis — diverticulum of the corpus extending cranially beyond the gastro-oesophageal junction. G = grenzfalte — bordering fold of tissue separating the glandular and non-glandular epithelia. I = incisura angularis — prominent angle on the lesser curvature of the stomach. O = oesophagus, D = duodenum. Fu, Py and Ca = fundic, pyloric and cardiac regions of the antrum respectively.



Legend

Glandular tissue	Non-papillated epithelium
Transition area	Papillated epithelium
Muscularis externa	Duodenal epithelium

Figure 1b Semi-diagrammatic drawing of photograph in Figure 1a (same lettering).

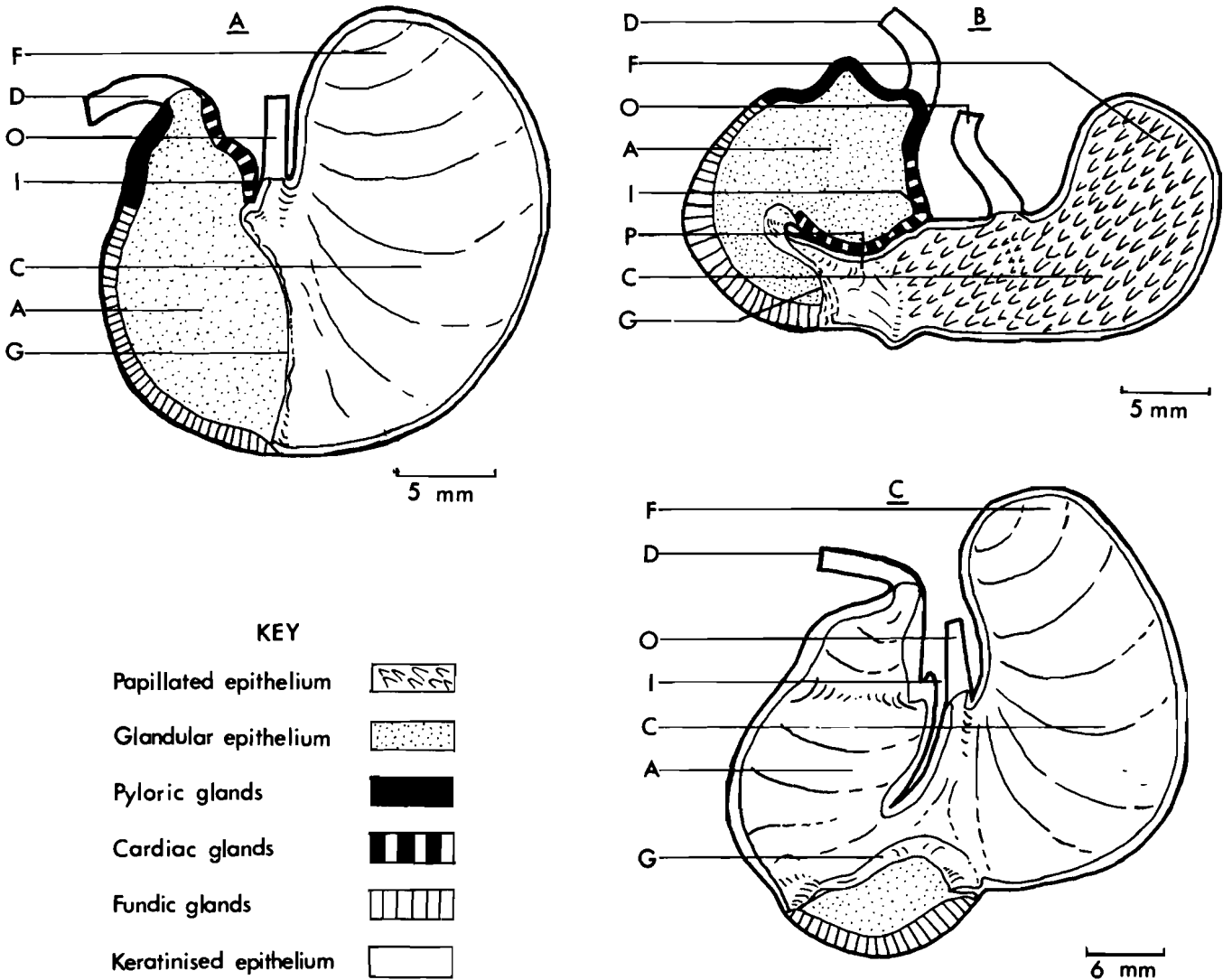


Figure 2 A generalized diagram of the three stomach types (modified after Carleton 1973). (A) unilocular hemiglandular, (B) bilocular hemiglandular (*M. albicaudatus*) and (C) bilocular discoglandular. Lettering as in Figure 1a.

and ‘advanced’ types (Figure 2). The proximal, non-glandular pars oesophagea consisted of a papillated corpus and a non-papillated pre-gastric pouch (PGP) (Figure 1). The glandular antrum was separated from the pars oesophagea by a bordering fold of tissue, the grenzfalte (Figure 1).

The oesophagus entered the mid-dorsal region of the corpus, which was enlarged by a diverticulum of the fornix ventricularis (Figure 1). Papillae, a few of which were bifurcate, were irregularly orientated in the corpus. A

constriction (the pre-gastric pouch — PGP) extended from the corpus adjacent to the PGP to the distal side of the grenzfalte (Figure 1).

The antrum was a glandular sac originating immediately distal to the grenzfalte. Its asymmetrical U-shape (the larger, distal, section of which lead directly to the duodenum) was due to an angular notch or incisura angularis (Figure 1). pH readings from the non-glandular and glandular regions, and papillae measurements are summarized in Table 3.

Table 3 pH values from the glandular and non-glandular regions of the stomach of *M. albicaudatus* and corpal papillary measurements

	pH value	Density	Length
Antrum	2,7 (SD = 0,29) (n = 10)	—	—
Corpus	4,6 (SD = 0,46) (n = 10)	—	—
Papillae	—	550/cm ² (SD = 114) (n* = 1 300, n = 10)	1,8 mm (SD = 0,45) (n* = 124, n = 10)

n* = number of samples examined; n = number of animals examined

Histology

With the exception of the epithelium, a typical mammalian stomach tissue plan (Dearden 1966, 1969; Madge 1975) was seen in *M. albicaudatus*. A thin serosa and muscularis externa comprising two smooth muscle layers, inner circular (stratum circulare) and outer longitudinal (stratum longitudinale), were present. Generally the muscularis externa was thicker in the corpus (where it supported a keratinized, papillated epithelium) than in the PGP or antrum. The stratum circulare was approximately four times thicker than the stratum longitudinale in the antrum, twice as thick in the corpus and in the fornix ventricularis the layers had equal thickness. The stratum circulare was exceptionally well developed at the pylorus and gastro-oesophageal junction where it formed the pyloric and oesophageal sphincters respectively (Figure 1a).

The oesophageal muscularis externa consisted of striated muscle (Figure 3), the outer longitudinal layer continued from the right side of the oesophagus to the incisura angularis. Longitudinal muscle on the left of the oesophagus penetrated the outer smooth muscle layer of the stomach so that a transitional region of both smooth and striated fibres occurred at the gastro-oesophageal junction. The oesophageal inner circular striated muscle layer changed to gastric smooth muscle immediately prior to the oesophageal sphincter (Figure 3).



Figure 3 The gastro-oesophageal junction; striated muscle layers (StM) of the oesophageal muscularis externa interdigitate with the gastric smooth muscle layers (SmM). The folded, keratinized oesophageal epithelium (OE) and the corpal papillated epithelium (E) are indicated.

A submucosa of loose connective tissue with nerve fibres and numerous blood vessels maintained a constant thickness in the corpus and PGP but was often absent from the antrum where the muscularis externa and mucosa were closely attached. The corpal muscularis mucosa was continuous with that of the oesophagus but was incomplete, being represented by an indistinct longitudinal, smooth muscle layer (particularly evident in the

fornix ventricularis). Inner circular and outer longitudinal smooth muscle fibres occurred in the muscularis mucosa in the antrum, except along the greater curvature where longitudinal muscle predominated. Few transverse fibres occurred in the middle of this layer at regular intervals.

Fine reticular connective tissue and elastin fibres constituted the lamina propria which had an irregular thickness in both the corpus (due to the folded epithelium) and in the antrum (where it extended between the glandular tissue) (Figure 4). In the antrum, the lamina propria also contained smooth muscle fibres from the underlying muscularis mucosa. Interlocking connective tissue and epithelial papillae, termed epithelial pegs by Hyden & Sperber (1965), were absent.

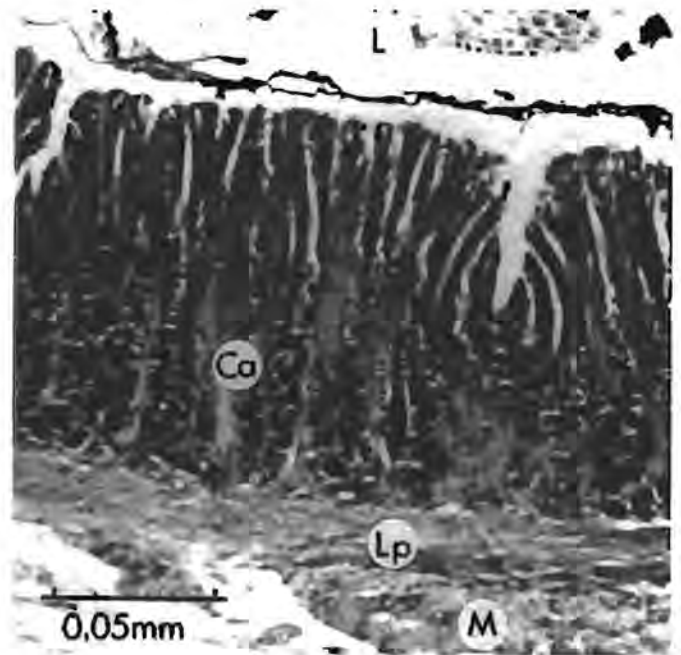


Figure 4 A longitudinal section through the cardiac region of the stomach. The lamina propria (LP) extends between the short, branched cardiac glands (Ca). L = lumen, M = muscle layers.

The pars oesophagea was lined by stratified, squamous epithelia. Keratinization had taken place through keratohyalin thus forming 'soft' keratin and all the layers typical of the mammalian epidermis (Jarrett 1973), with the exception of the stratum lucidum, were well represented in this region. A folded corpal epithelium (FCE) lined the corpus, and between the folds were keratinized papillae (Figure 5) which differed from those of the rumen by lacking a connective tissue core, or swollen cells in the superficial layers (Hofmann 1973). The stratum corneum constituted the main part of the papillae and there was an extensive stratum spinosum compared to the FCE (Figure 5) and PGP (Figure 7). Masses of symbiotic bacteria penetrated the horny layer and formed numerous microhabitats throughout the papillae length (Figure 6). This was not seen in the adjacent FCE where bacteria were fewer and formed a thin surface layer (Figure 5).

The junction between the corpus and PGP was marked by the termination of the papillated epithelium. PGP epithelium was folded and had a thicker malpighian layer

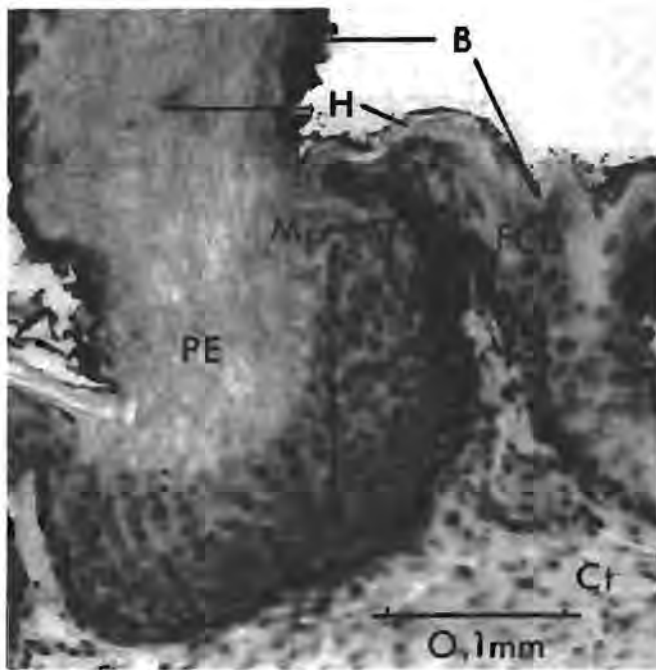


Figure 5 Longitudinal section through the FCE and papillary epithelium (PE). Note the difference in thickness between the malpighian layers (Mp), horny layers (H) and bacterial covering (B) of the FCE and PE regions. Ct = connective tissue.

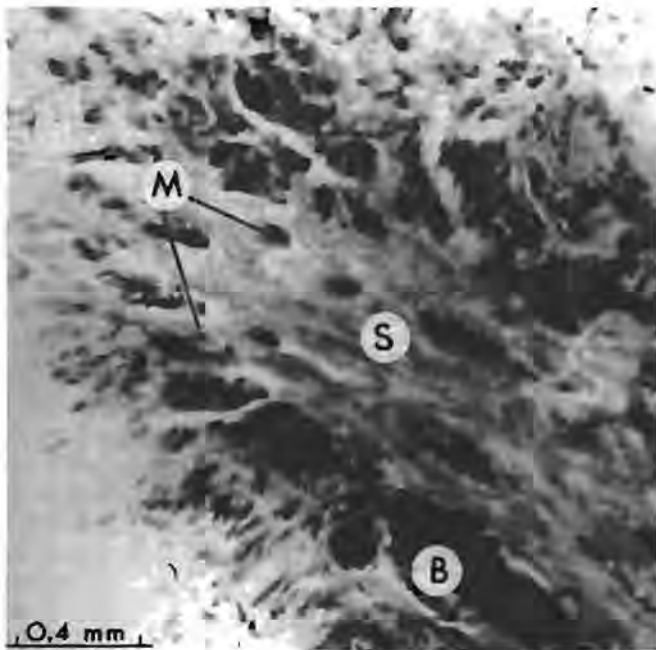


Figure 6 A high power micrograph of a section through the tip of a papilla showing penetration of the keratin by the bacteria (B) and resulting microhabitats (M). S = stratum corneum.

and more distinct granular layer than the FCE but was otherwise histologically similar (Figure 7). Bacterial colonization of the PGP was also similar to that of the FCE. The *grenzfalte*, separating the glandular and non-glandular areas, was a keratinized flap of tissue with a muscularis mucosa core. This flap appeared to be continuous with the thickened glandular epithelium on the distal side (i.e. keratinized on the side of the PGP and glandular on the opposite side) but this was not the case as keratinization occurred on both sides of the *grenzfalte* (Figure 8).

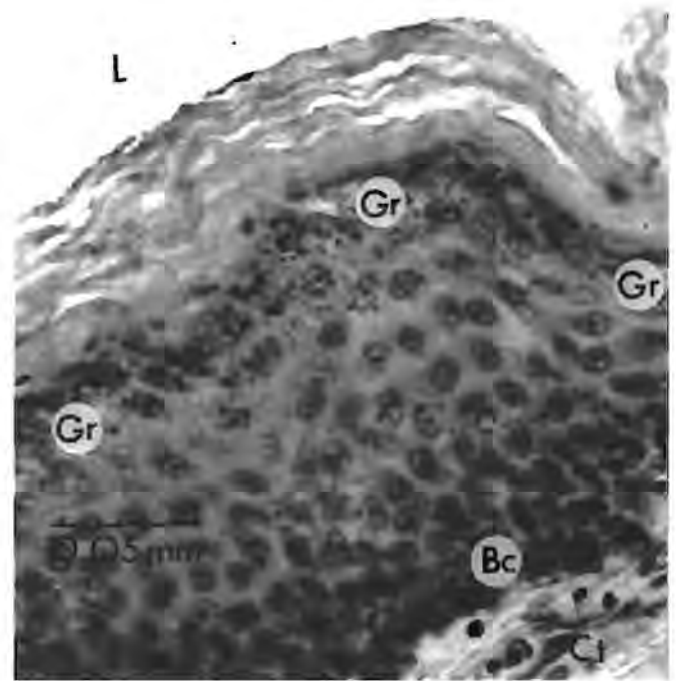


Figure 7 Section through the PGP epithelium showing the distinct granular layer (Gr) and basophilic basal cells (Bc). Ct = connective tissue, L = lumen.

Distal to the *grenzfalte* was the antrum which was histologically divisible into cardiac, pyloric and fundic regions with short transition areas between each (Figure 1). Along the lesser curvature, extending from the *grenzfalte*, was the cardiac region (Figures 1 & 4) with short, branched glands which increased in length towards the pylorus (Figure 10). Mucus-secreting glands with wide foveola occurred in the pyloric region and chief cells were found at the base of the gland in the pyloric/fundic transition area. Long tubular, fundic glands with narrow foveolae lined the greater curvature and extended to the *grenzfalte* (Figures 1, 8 & 9). These glands presented a typical mammalian cytology; that is, cuboidal neck cells above mucous neck cells, followed by chief cells at the base. Parietal cells occurred throughout the gland but predominated in the basal region (Figure 9).

Histochemistry

Hematoxylin and eosin (H & E) and toluidene blue stains demonstrated a lack of nuclei in the stratum corneum but detected the presence of keratohyalin granules in the stratum granulosum. These features indicated complete keratinization and formation of 'soft' keratin. Lipid droplets were not revealed in the corpal epithelium although oil red O and Sudan black stains were used. Tissues increased in stain intensity towards the stratum corneum suggesting an increase in lipid content.

The slight PAS positive reaction in the corpal basal and spinous cell cytoplasm was probably indicative of glycogen, important in the keratinization process. The lamina propria and the bacteria were strongly PAS positive. Gastric mucin was present in the lumens of the cardiac and pyloric glands but only in the fundic gland foveolae. No PAS reaction or toluidene blue metachromasia occurred in the corpus, indicating an absence of mucus in the pars oesophagea.

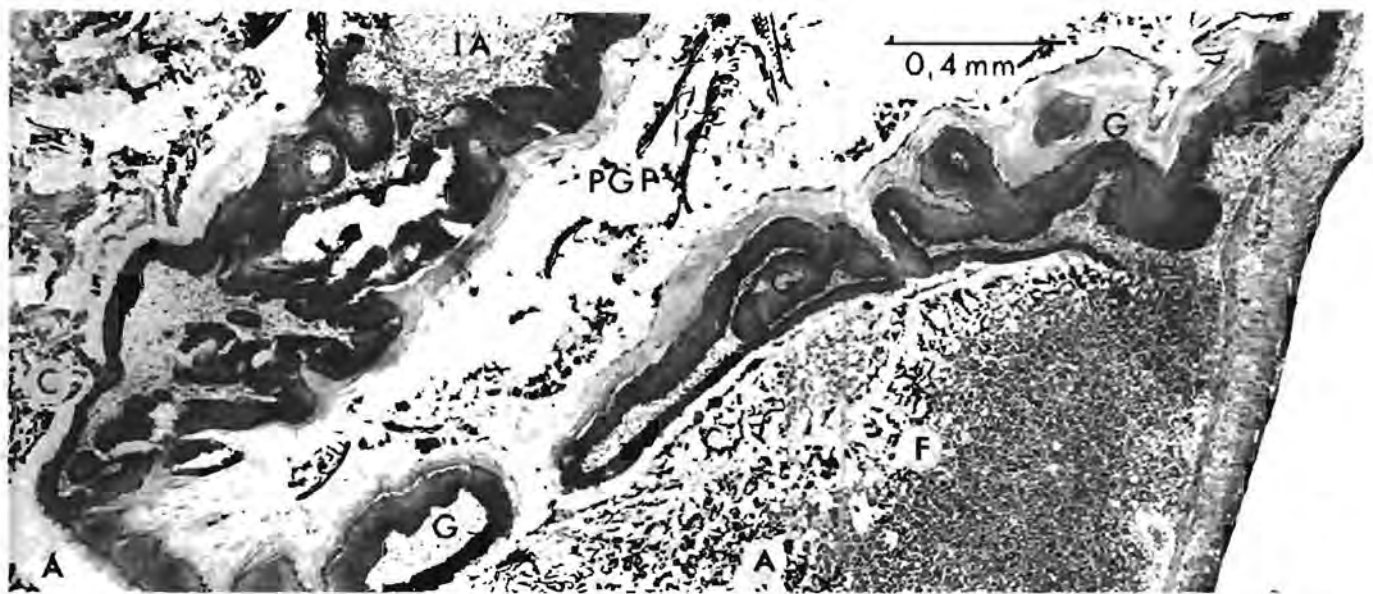


Figure 8 The keratinized grenzfalte (G) separating the PGP and antrum (A), extends from the greater curvature of the stomach to the incisura angularis (IA). F = fundic and C = cardiac epithelia.

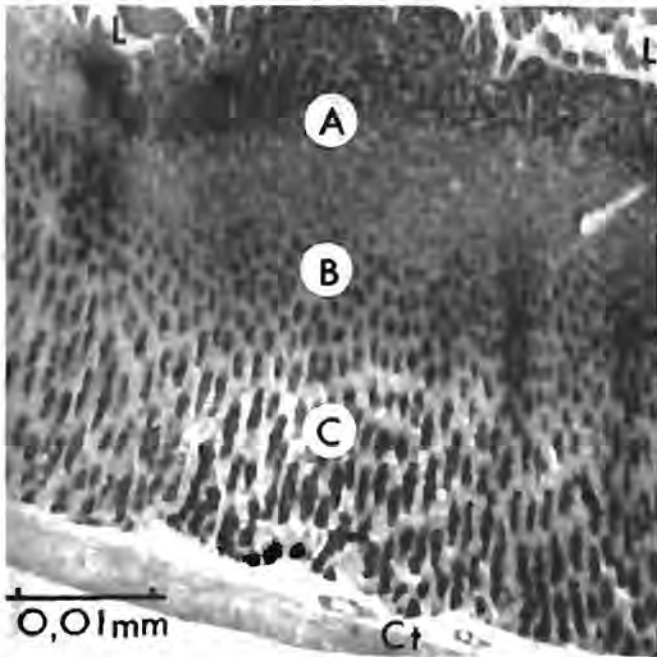


Figure 9 Longitudinal section through the fundic glands. Three regions, characterized by different cells are present; A = surface mucus and mucus neck cells, B = basophilic chief cells, C = acidophilic parietal cells and basophilic chief cells. Ct = connective tissue, L = lumen.

The presence of sulphur groups in the superficial epithelial layers of the pars oesophagea was confirmed by increased intensity of the aldehyde fuchsin and ferric ferrocyanide stains towards the stratum corneum. The stratum corneum stained positively with both stains.

Scanning electron microscopy (SEM)

Sterile rats were used to examine the papillae because numerous bacteria in conventional rats completely obscured surface detail. The FCE epithelium was visible in conventional rats because of the fewer bacteria in this region. SEM revealed that the desquamating cells of the papillae were smaller than those of the FCE (Figure 11) and that bacteria occurred in areas (microhabitats) between the small squames (Figure 12). Similar bacterial colonization

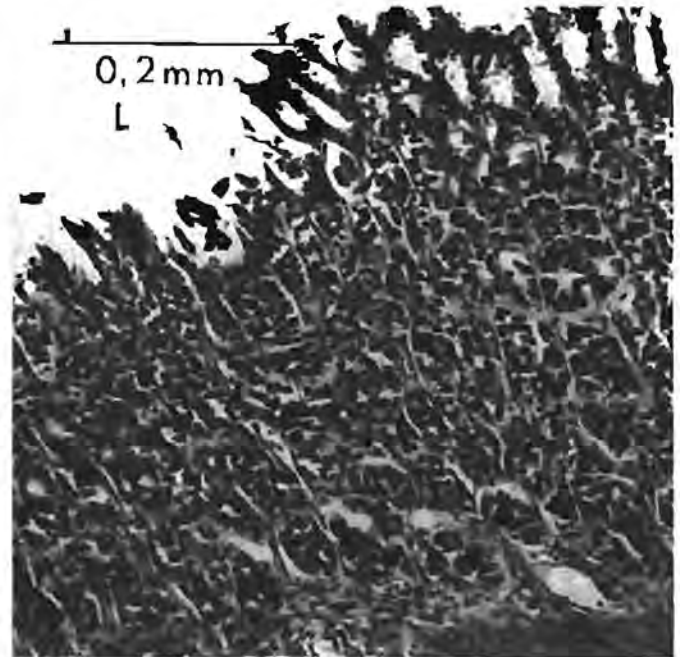


Figure 10 Longitudinal section through the mucus cells of the pyloric region. L = lumen.

did not occur among the larger FCE squames. Among the irregularly orientated FCE squames there was a compact, regular epithelium (Figure 13) not seen in the papillae. PGP epithelium was seen in conventional rats and was similar to the compact epithelium of the FCE (Figure 13).

Foveolae of the gastric glands were visible in the antrum (Figure 14) unless obscured by mucus. The presence of occasional, isolated bacteria and absence of other micro-organisms, as noted in histological sections, was confirmed. Microvilli covered the surface epithelial cells of the cardiac (Figure 14) and pyloric regions.

Transmission electron microscopy

TEM studies of the pars oesophagea confirmed the light microscope findings and a normal sequence of keratini-

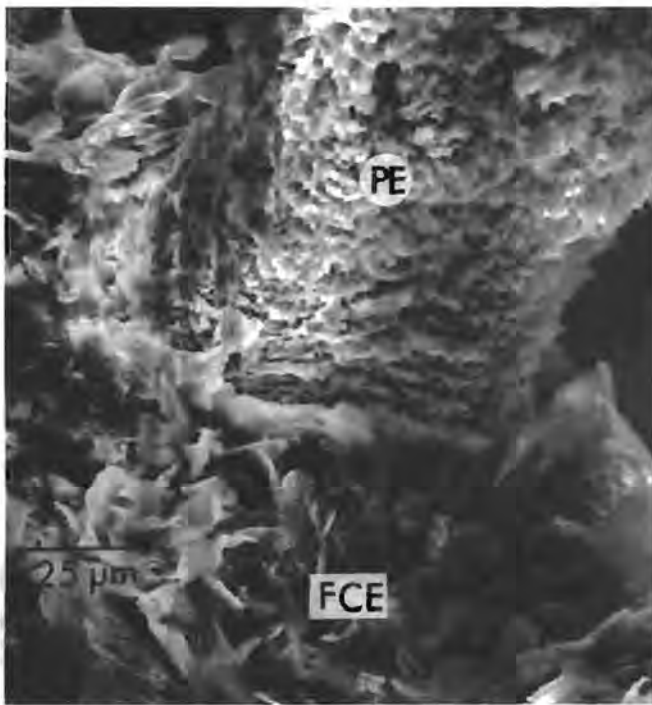


Figure 11 A scanning electron micrograph of the corpus showing the base of a papilla and the FCE. The desquamating epithelial cells of the FCE are larger than the papillary cells (PE). (Specially treated rat.)

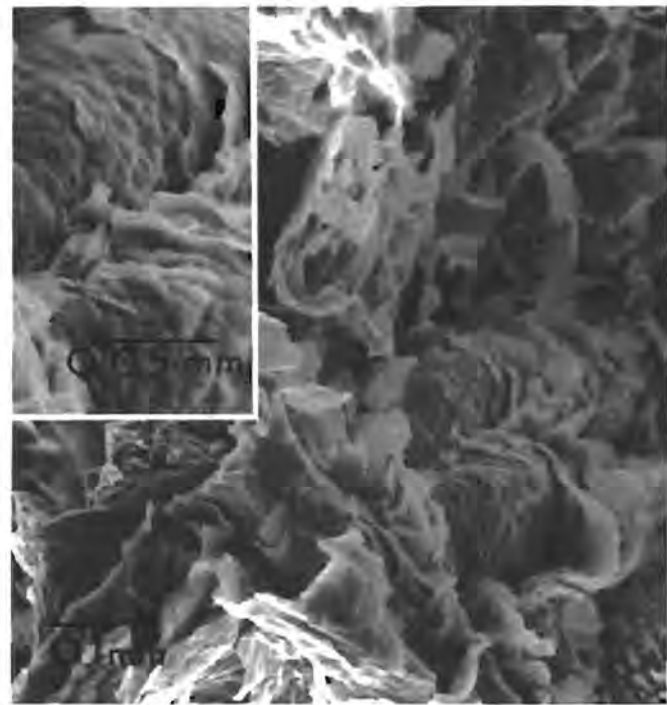


Figure 13 The surface of the FCE from a specially treated rat. The regular compact epithelium is seen left and below centre. The inset shows this area at higher magnification.

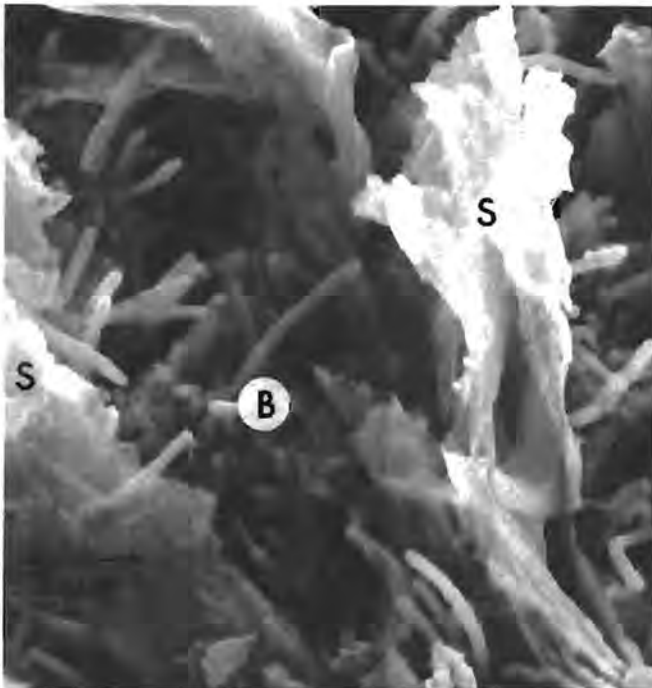


Figure 12 A microhabitat between desquamating cells (S) of a papilla. Note the presence of bacilli and cocco-bacilli (B). (Specially treated rat.)



Figure 14 Surface mucus cells with microvilli (M) around the foveolus (F) of a cardiac gland. (Sterile rat.)

zing epithelium was seen although the papillary epithelia, FCE and PGP epithelia had slight ultrastructural differences.

In the stratum basale an electron translucent space was present between the basement and plasma membranes in the pars oesophagea. The papillae, FCE and PGP epithelia had characteristic microvilli extending from the basal cells into wide intercellular spaces. The plasma membrane was thin and highly convoluted (Figure 15). Mitochondria, abundant in the papillary basal cells (Figure 15) were comparatively few in the tonofilament-rich PGP

and FCE. Golgi and rough endoplasmic reticuli (RER) were rare.

The stratum spinosum was characterized by an increase in desmosomes and small electron dense granules (probably ribosomes), and tonofilaments and cytoplasmic oval bodies (COB) became apparent (Figure 16). COB were present in all spinous layers and were often membrane-bound with an electron translucent internal structure; few possessed an electron dense or laminated structure. Cellular degeneration and flattening occurred in the superficial regions (Figure 16). This layer was extensive in

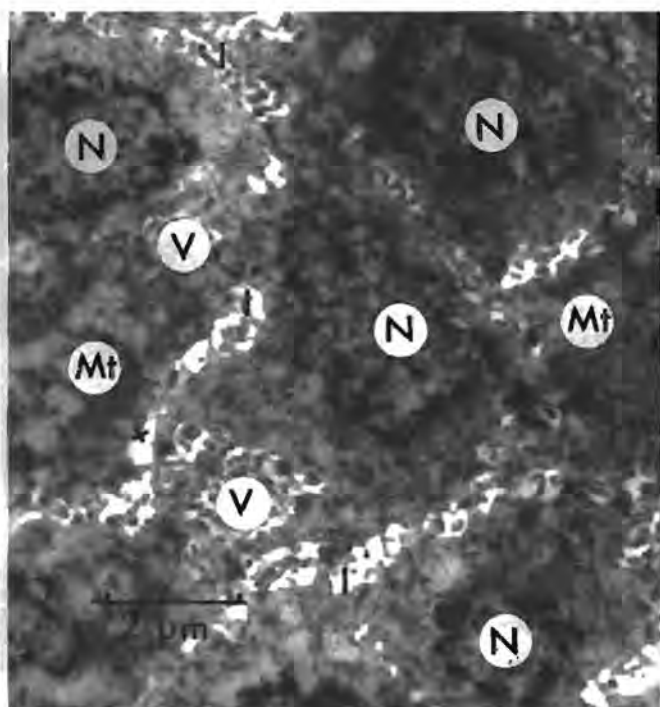


Figure 15 A transmission electron micrograph of the papillary epithelium. Characteristic, wide intercellular spaces (I), microvilli (V) and the thin, convoluted plasma membrane (X) are indicated. The small, opaque granules are ribosomes. Mt = mitochondria.

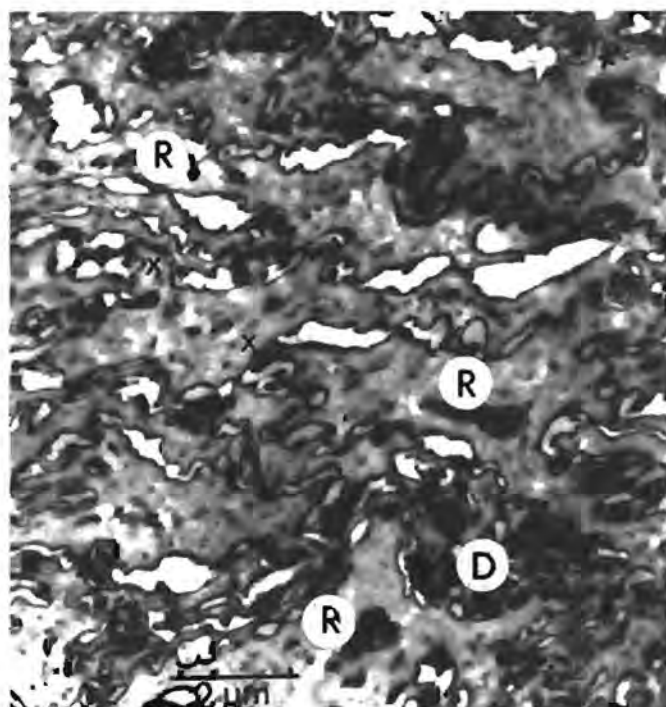


Figure 17 The central area of a papilla. Note the numerous keratin fibrils and cellular interdigitations. R = cellular remnants, D = degenerating desmosomes (squamosomes), X = electron-dense intercellular material.

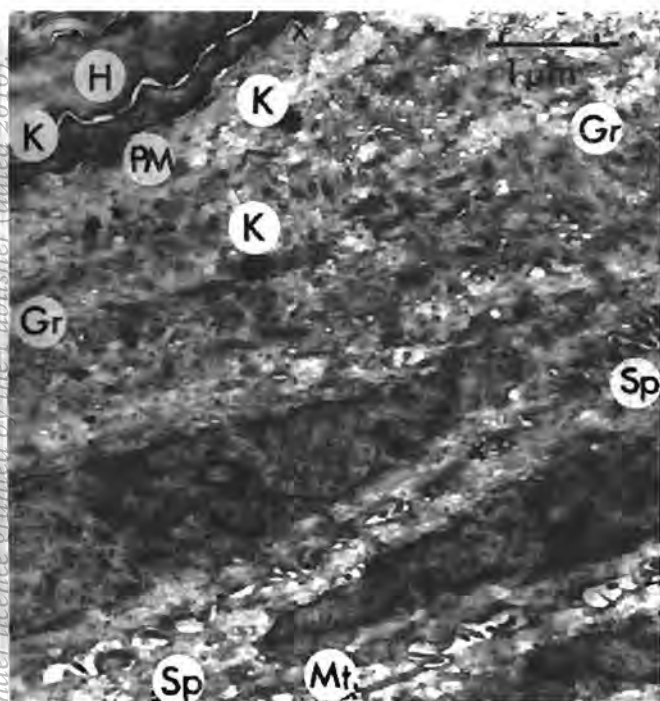


Figure 16 A micrograph showing the stratum spinosum (Sp), granulosum (Gr) and corneum (H). Cellular flattening is marked in the upper spinous layers. Fine particle aggregations occur around the keratohyalin granules (K). The thickened plasma membrane (PM) is shown in the stratum corneum. Mt = mitochondria, X = desmosome.

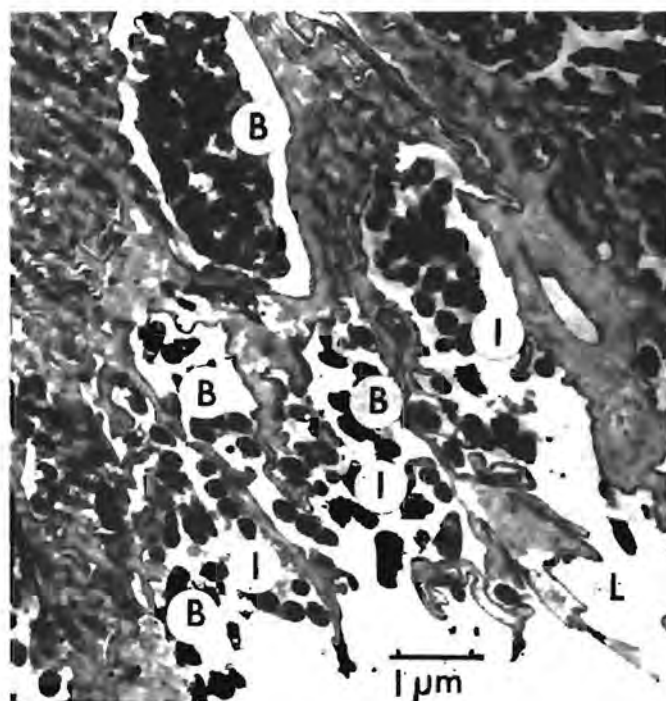


Figure 18 The periphery of a papilla from a specially treated rat. The horny cells are similar to those in Figure 17 although no nuclear remnants are present. Bacteria (B) occur in the widened intercellular spaces (I). L = lumen.

the papillae compared to the stratum spinosum of the PGP and FCE, and spinous cellular changes (common throughout the FCE and PGP layers) were only apparent in the upper papillary stratum spinosum. Cellular degeneration was advanced in the stratum granulosum and the cells contained numerous small, electron-dense granules

(which aggregated around the keratohyalin granules — KG) and numerous tonofilaments (Figure 16). Desmosomes and some degenerating nuclei were also present in the superficial layers (Figure 16).

The junction between the strata granulosum and corneum was marked by an abrupt thickening of the horny

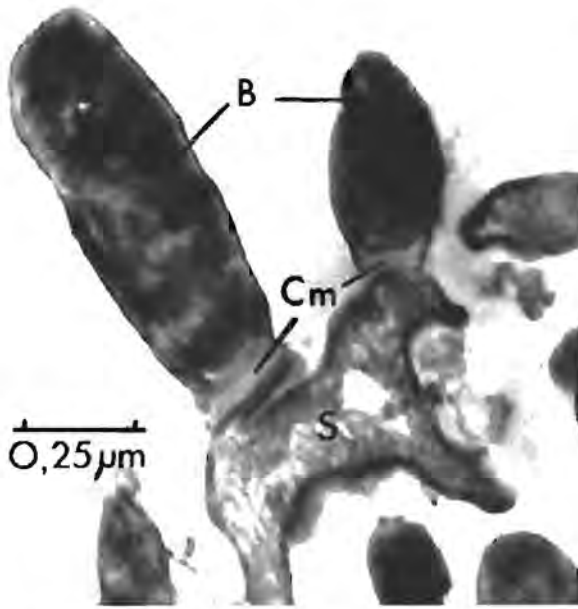


Figure 19 Bacterial attachment to desquamating papillary cells (S). B = bacteria, CM = bacterial capsular membrane.

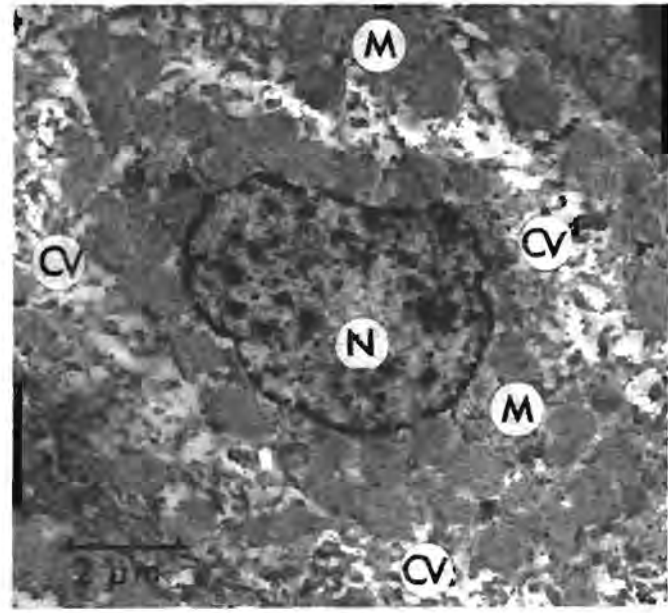


Figure 21 A section through a parietal cell from a fundic gland. Note the canaliculus with microvilli (CV) around the nucleus (N) and the abundance of mitochondria (M).

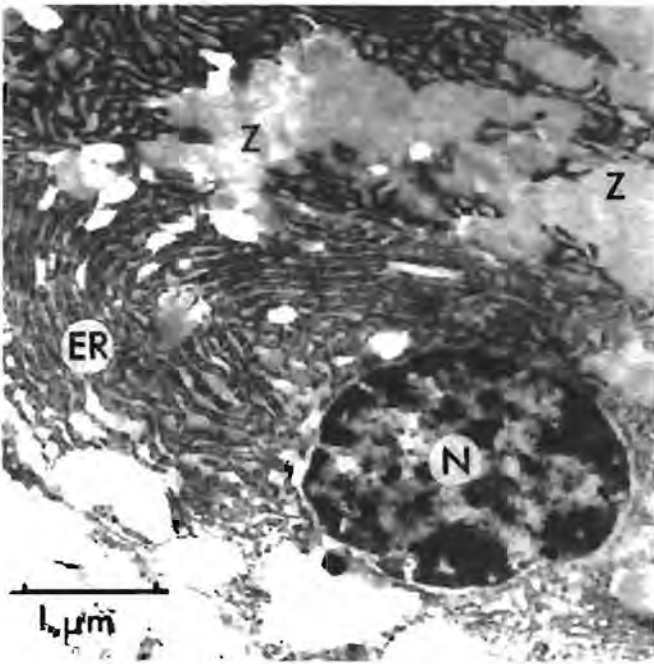


Figure 20 A section through a chief cell from a fundic gland. Features typical of these cells are apparent: Z = zymogen granules, ER = endoplasmic reticulum, N = nucleus.

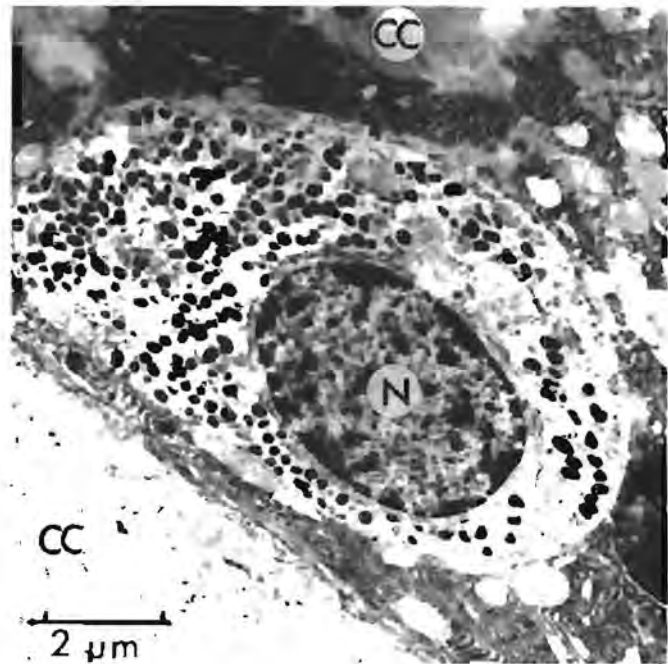


Figure 22 An enterochromaffin cell surrounded by chief cells (CC). Note the electron-dense granules and the light cytoplasm of the endocrine cell. N = nucleus.

cells' plasma membrane (Figure 16). The lower horny cells contained keratin fibrils, KG, and few desmosomes (Figure 16). Other organelles had degenerated. Cells of the mid and superficial stratum corneum contained randomly orientated keratin fibrils in an amorphous matrix and some cellular remnants (Figure 17). Desmosomes had degenerated to form squamosomes (Allen & Potten 1974) and some electron-dense material was present in the intercellular spaces (Figure 17). Desquamating cells showed much interdigitation, particularly in the papillae (Figure 17) and in the papillary periphery the intercellular spaces widened. Bacterial colonization of these wide intercellular spaces corresponded to the microhabitats seen in SEM

micrographs (Figures 12 & 18). Some bacteria were attached to the desquamating cells by means of a thickened capsular layer (Figure 19). TEM observations confirmed the presence of surface epithelial cells (with microvilli), chief cells (Figure 20) and parietal cells (Figure 21). Endocrine cells (enterochromaffin cells) were present in the fundic region (Figure 22).

Discussion

The corpus of *M. albicaudatus* has a non-glandular, stratified squamous epithelium modified to form keratinized papillae while the antrum possesses cardiac, pyloric and fundic glands. Carleton (1973) recognized a series of

rodent stomach types from the simple unilocular hemiglandular to the complex bilocular discoglandular type. The gastric morphology of *M. albicaudatus* attains the bilocular condition but shows no overt discoglandular arrangement of the secretory epithelia. The term bilocular hemiglandular is adopted for such a stomach which resembles that of *C. gambianus* (Caiman *et al.* 1960).

Although a discoglandular arrangement is not apparent, *M. albicaudatus* has a papillated bilocular hemiglandular stomach which may be approaching a papillated discoglandular condition. An increase in cardiac, and cardiac/fundic transitional glands (at the expense of pyloric glands, Bensley 1905), restriction of the fundic area and subsequent replacement of cardiac glands by keratinized epithelium generates the modified bilocular discoglandular condition. The position and area occupied by fundic and cardiac glandular epithelia in *M. albicaudatus*, the compensatory increase in the length of the fundic glands (Luthje 1976) and the fact that the *grenzfalte* is keratinized and not glandular (*cf.* Bensley 1905) is indicative of trends towards the modified digastric stomach type.

Peters & Gärtner (1973) found that *Rattus norvegicus* and *Mus musculus* have a thin, elastic forestomach and a muscular, thick-walled glandular stomach; the lack of forestomach musculature implies that mechanical preparation of food in this organ cannot be similar to that of ruminants (Krzywaneck 1927). *M. albicaudatus*, however, has a thicker muscularis externa in the corpus than in the antrum, in addition to a layer of striated muscle extending from the oesophagus to the *incisura angularis*, suggesting that mechanical preparation of food in the forestomach of *M. albicaudatus* is more important than in the rodents examined by Peters & Gärtner (1973).

Epithelial stratification, with keratohyalin granules in the stratum granulosum, indicates that the pars oesophageal epithelium of *M. albicaudatus* has undergone 'soft' keratinization. Spearman (1977) and Matoltsy (1962) reviewed the process of epidermal keratinization which parallels the keratinization of the non-glandular region of the stomach of *M. albicaudatus*. The papillae show a slightly different type of keratinization to the FCE and PGP epithelium; the thick papillary stratum corneum resembles the pathological epidermal condition termed hyperkeratosis. However, this condition is not pathological in *M. albicaudatus* but is a normal, physiological adaptation whereby symbiotic bacteria are provided with ecological niches. The term physiological hyperkeratosis is thus suggested for this type of keratinization; orthokeratin is suggested for the 'soft' keratin of the FCE and PGP.

The extensive stratum corneum of the papillae is generated by a high mitotic rate in the basal cells. The papillary epithelium, although not possessing epithelial pegs, shows a thickening of the basal layers and may parallel phase two type epidermis which is characterized by a high mitotic rate resulting in a thickened epithelium (Bullough 1975). The abundance of mitochondria in the basal cells may account for the high mitotic rate. (Rumen epithelia also possess numerous basal cell mitochondria, but in contrast to *M. albicaudatus*, these are important in absorption of rumen metabolites.) The FCE and PGP epithelium has a unicellular basal layer and thin epithelium,

thus paralleling phase one type epidermis (Bullough 1975).

The precise adaptive functions of the stomach of *M. albicaudatus* are unknown. It has been proposed that sacculization of certain cricetid stomachs permits pH to remain near neutrality in the corpus allowing for continued salivary α -amylase activity (Carleton 1973), which has also been reported for the non-glandular forestomach of the rat (Kunstyr, Peters & Gärtner 1976; Peters & Gärtner 1973). Amylase (optimal pH 7) in this region would, however, be partially denatured by the low pH and would not have optimal activity. The acidity is caused by microbial metabolites, as both pH and amylase activity increase in germ-free rats (Kunstyr *et al.* 1976). Kunstyr *et al.* (1976) therefore considered the forestomach microflora of the rat detrimental to starch digestion. Inner regions of the chyme may, however, have a higher pH than that of the periphery allowing for some degree of amylolysis (Peters & Gärtner 1973). An acidic pH (4.6) occurs in the corpus of *M. albicaudatus* and thus reduction of amylase activity is probable. The acid conditions and presence of numerous bacteria on the corpal papillae suggest that a reservoir with amylolytic activity, is not the primary function of the corpus although it is possible for some starch hydrolysis to occur if the food has a slow passage through the stomach.

The papillae are considered to play an integral role in the corpus but owing to the absence of vascularization and presence of keratinization they are not absorptive, unlike rumen papillae (Hyden & Sperber 1965; Lavker, Chalupa & Dickey 1969; Henrikson 1970). The intimate association between the papillary stratum corneum and numerous bacteria in healthy *M. albicaudatus* suggests a symbiotic relationship. The evolution of the papillae cannot be readily explained by assuming that the bacteria are parasitic or physiologically detrimental to the host. The bacteria on the FCE and PGP epithelium constitute a separate autochthonous flora, characteristic of many rodents (Savage 1977).

An understanding of the mechanisms and processes of this symbiotic relationship will only be gained by studies of digestive physiology and microbial function. It is possible that protein-rich bacteria are digested by *M. albicaudatus*. However, it has been demonstrated that *Rattus norvegicus* and *Mus musculus* do not obtain protein from a gastric bacterial source (Gärtner & Pfaff 1979). Ehle & Warner (1978) suggest that microbial activity in the forestomach of *Mesocricetus auratus*, may assist that in the caecum, and improve forage cell wall digestibility. This process contrasts with Vorontsov's functional compensation theory (1961) but Perrin & Curtis (1980) noted that concurrent morphological modification of forestomach and caecum may be associated with different or complementary digestive processes. The rodent caecum is undoubtedly important for microbial fermentation in many species (McBee 1971). However, the papillated corpus, symbiotic bacteria, stomach sacculization and simple caecum of *M. albicaudatus* suggest that it is the forestomach that initiates and predominates in microbial fermentation processes. Similar conclusions were drawn by Sakata & Tamate (1976) and Hoover, Mannings & Sheerin (1969) when studying *M. auratus*.

In conclusion, the non-glandular corpus of *M. albicaudatus*

datus is lined with keratinized epithelia, and FCE, papillary and PGP epithelia are present, each with different mitotic rates and thicknesses. The corpal papillae maximize surface area for attachment of symbiotic bacteria, possibly important in carbohydrate fermentation. It is believed that these bacteria, in smaller numbers, would not predispose a dietary advantage to the host; the papillae thus being crucial for the symbiotic relationship. The corpus may have other secondary functions. Ehle & Warner (1978) noted that the effectiveness of forestomach fermentation is decreased by the rapid emptying rate of stomach contents. The papillae of *M. albicaudatus* may slow the rate of gastric ingesta flow causing food to be subjected to microbial activity for a longer period and thus increasing the effectiveness of fermentation. Finally, the findings of Kunstyr *et al.* (1976) with *R. norvegicus* propound that increased starch digestion may occur in the corpus of *M. albicaudatus*. The antrum retains cardiac, fundic and pyloric glands for proteolytic digestion.

M. albicaudatus has developed specialized herbivorous adaptations and retained the ability to digest protein. Specializations of this cricetid are partially offset by the reproductive potential of murids (Perrin 1980). Studies are underway to determine digestive efficiency in relation to the role of the papillary bacteria.

Acknowledgements

We thank the staff of the Rhodes University Electron Microscope Unit, Mr R.H.M. Cross and Mr A. Bruton for their constructive ideas and invaluable technical assistance. Thanks are also due to Professor W.H. Gerneke and Mr D. Ranchhod for advice on histological interpretation and histological technique. This study was funded by a CSIR grant.

References

- ALLEN, T.D. & POTTEN, C.S. 1974. Fine structural identification and organization of the epidermal proliferative unit. *J. Cell Sci.* 15: 291–319.
- ANDERSON, J.F. 1951. Techniques for the preservation of three-dimensional structure for the electron microscope. *Trans. N. Y. Acad. Sci.* 13: 130–134.
- AYOUB, P. & SHKLAR, G. 1963. A modification of the Mallory connective tissue stain as a stain for keratin. *J. Oral Surg.* 16: 580–581.
- BENSLEY, R.R. 1905. The cardiac glands of mammals. *Am. J. Anat.* 2: 105–156.
- BULLOUGH, W.S. 1975. Mitotic control in adult mammalian tissues. *Biol. Rev.* 50: 99–127.
- CAIMAN, R., QUENUM, A., KERREST, J. & GOUEFFON, S. 1960. Considerations sur l'estomac de *Cricetomys gambianus*. *C. R. Searl Soc. Bio., Paris.* 154: 1578–1579.
- CARLETON, M.D. 1973. A survey of gross stomach morphology in New World Cricetinae (Rodentia, Muroidea) with comments on functional interpretations. *Museum of Zoology, University of Michigan.* 146: 1–42.
- CROSS, R.H.M. 1979. The preparation of biological material for electron microscopy. Unpublished manual of the Rhodes University Electron Microscope Unit.
- DEARDEN, L.C. 1966. Histology of the gastro-esophageal junction in certain microtine rodents. *J. Mammal.* 47: 223–229.
- DEARDEN, L.C. 1969. Stomach and pyloric sphincter histology in certain microtine rodents. *J. Mammal.* 50: 60–68.
- EHLE, F.R. & WARNER, R.G. 1978. Nutritional implications of the hamster forestomach. *J. Nutr.* 108: 1047–1053.
- GÄRTNER, K. & PFAFF, J. 1979. The forestomach in rats and mice, a food store without bacterial protein digestion. *Zbl. Vet. Med. A.* 26: 530–541.
- HENRIKSON, R.C. 1970. Ultrastructure of ovine ruminal epithelium and localization of sodium in the tissue. *J. Ultrastruc. Res.* 30: 385–401.
- HOFMANN, R.R. 1973. The ruminant stomach. East African Literature Bureau, Nairobi.
- HOOVER, W.H., MANNINGS, C.L. & SHEERIN, H.E. 1969. Observations on digestion in the golden hamster. *J. Anim. Sci.* 28: 349–352.
- HUMASON, G.L. 1967. Animal tissue techniques. Freeman & Co., San Francisco.
- HYDEN, S. & SPERBER, I. 1965. Electron microscopy of the ruminant forestomach. In: Physiology of digestion in the ruminant. (ed.) Dougherty, R.W. Butterworths, Washington.
- JARRETT, A. 1973. The physiology and pathophysiology of the skin. Academic Press, London.
- KRZYWANIEK, W. 1927. Vergleichende Untersuchungen über die mechanik der Verdauung II Röntgenologische Studien am omnivoren Nager (Ratte). *Arch. Tierheilk.* 55: 523–536.
- KUNSTYR, I., PETERS, K. & GÄRTNER, K. 1976. Investigations on the function of the rat forestomach. *Lab. Anim. Sci.* 26: 166–170.
- LANDRY, S.O. 1970. The rodentia as omnivores. *Q. Rev. Biol.* 45: 351–372.
- LAVKER, R., CHALUPA, W. & DICKEY, J.F. 1969. An electron microscope investigation of rumen mucosa. *J. Ultrastruc. Res.* 28: 1–15.
- LUNA, L. 1968. Manual of histologic staining methods of the armed forces institute of pathology. McGraw-Hill, New York.
- LUTHJE, V.B. 1976. Vergleichende funktionell-anatomische und histochemische Untersuchungen am Magen von mitteleuropäischen Murinae (Murray 1866) und Microtinae (Millar 1896) (Rodentia). *Zool. Jb. Anat. Bd.* 96: 451–512.
- MADGE, D.S. 1975. The mammalian alimentary system, a functional approach. Edward Arnold, London.
- MATOLTSY, A.G. 1962. In: Fundamentals of keratinization. (Eds.) Butcher, E.O. & Sognnaes, R.F. Am. Ass. Advance. Sci., Publ. 70. Washington D.C.
- McBEE, R. 1971. Significance of intestinal microflora in herbivory. *Ann. Rev. Ecol. Syst.* 2: 165–176.
- MOIR, R.J. 1968. Ruminant digestion and evolution. In: Handbook of physiology, Section 6. The alimentary canal. Vol. V., Rumen physiology, pp. 2673–2694.
- PERRIN, M.R. 1980. Ecological strategies of two co-existing rodents. *S. Afr. J. Sci.* 76: 487–491.
- PERRIN, M.R. & CURTIS, B.A. 1980. Comparative morphology of the digestive system of 19 southern African Myomorph rodents in relation to diet and evolution. *S. Afr. J. Zool.* 15: 22–33.
- PETERS, K. & GÄRTNER, K. 1973. Untersuchungen zur Funktion des Vormagens der Muriden 1. Passage fester und flüssiger Futterbestandteile, pH-werte und α -amylaseaktivität im Vormagen der Ratte. *Zbl. Vet. Med. A.* 20: 233–243.
- SAKATA, T. & TAMATE, H. 1976. Light and electron microscopic observation of the forestomach mucosa in the golden hamster. *Tohoku J. agric. Res.* 27: 26–39.
- SAVAGE, D.C. 1977. Microbial ecology of the gastro-intestinal tract. *Ann. Rev. Microbiol.* 31: 107–133.
- SPEARMAN, R.I.C. 1977. Keratins and keratinization. *Symp. Zool. Soc. Lond.* 39: 335–352.
- SUMNER, A.T. & SUMNER, B.E.H. 1969. A laboratory manual of microtechnique and histochemistry. Blackwell Scientific Publications, Oxford.
- VORONTSOV, N.N. 1961. Variation in the transformation rates of organs of the digestive system in rodents and the principle of functional compensation. *Dohlady Akad. Nauk. SSSR*, 136: 1494–1497. Eng. trans. in *Evolutionary Morphology Biol. Sci. Section.* 136–138: 49–52.
- VORONTSOV, N.N. 1962. The ways of food specialization and the evolution of the alimentary system in Muroidea. In: *Symp. Theriol. Publ. House Czech. acad. Sci.* pp. 360–377.